

# Dynamic Alignment and Exact Scaling Laws in MHD Turbulence

Stanislav Boldyrev,<sup>1</sup> Joanne Mason,<sup>2</sup> and Fausto Cattaneo<sup>2</sup>

<sup>1</sup>*Department of Physics, University of Wisconsin at Madison,  
1150 University Ave, Madison, WI 53706; boldyrev@wisc.edu*

<sup>2</sup>*Department of Astronomy and Astrophysics, University of Chicago, 5640 S. Ellis Ave,  
Chicago, IL 60637; jmason@flash.uchicago.edu; cattaneo@flash.uchicago.edu*

(Dated: May 10, 2006)

The Kolmogorov theory of hydrodynamic turbulence yields an exact relation for the third-order longitudinal velocity structure function,  $\langle \delta v_L^3(r) \rangle = -4/5 \epsilon r$ , where  $\delta v_L(r) = [\mathbf{v}(\mathbf{x}+\mathbf{r}) - \mathbf{v}(\mathbf{x})] \cdot \mathbf{r}/r$  and  $\epsilon$  is the rate of energy dissipation. One therefore expects the velocity scaling  $\delta v(r) \propto r^{1/3}$ , which leads to the Kolmogorov energy spectrum  $E(k) \propto k^{-5/3}$ . In 1998, Politano and Pouquet found that in magnetohydrodynamic turbulence certain third-order structure functions scale linearly with  $r$ . This appears to suggest that the spectrum of MHD turbulence also has the Kolmogorov scaling. However, recent high-resolution direct numerical simulations suggest that the spectrum is  $E(k) \propto k^{-3/2}$ . Here we propose that this apparent contradiction is a manifestation of the phenomenon of scale-dependent dynamic alignment recently discovered in MHD turbulence in [10, 11, 12].

PACS numbers: 52.30.Cv, 95.30.Qd

## INTRODUCTION

It is well known that the Kolmogorov theory for isotropic incompressible hydrodynamic turbulence yields the following exact relation for the third order longitudinal structure function of the velocity field in the inertial range (see, e.g., [1]):

$$\langle \delta v_L^3(\mathbf{r}) \rangle = -\frac{4}{5} \epsilon r. \quad (1)$$

Here  $\delta \mathbf{v}(\mathbf{r})$  is the velocity difference between two points separated by the vector  $\mathbf{r}$ ,  $\delta v_L(\mathbf{r}) = \delta \mathbf{v}(\mathbf{r}) \cdot \mathbf{r}/r$  is its longitudinal component and  $\epsilon$  is the rate of energy supply to the system at large scales. In a stationary state, it coincides with the rate of energy cascade toward small dissipative scales, and with the rate of energy dissipation. If one further assumes that the fluctuations are not strong compared to the rms value of  $\delta \mathbf{v}(\mathbf{r})$ , and that  $\delta v(r) \sim \delta v_L(r)$ , one can dimensionally estimate from (1) that  $\langle \delta v^2(\mathbf{r}) \rangle \propto r^{2/3}$ . The Fourier transform of the latter expression then leads to the Kolmogorov spectrum of turbulence,  $E(k) \propto k^{-5/3}$ .

Interestingly, analogous relations hold for isotropic magnetohydrodynamic turbulence. Writing the fluctuating magnetic field and velocity field ( $\mathbf{v}$  and  $\mathbf{b}$ , respectively) in terms of the Elsässer variables  $\mathbf{z} = \mathbf{v} - \mathbf{b}$  and  $\mathbf{w} = \mathbf{v} + \mathbf{b}$ , Politano & Pouquet [2, 3] derived

$$S_{3L}^w(r) \equiv \langle \delta z_L (\delta \mathbf{w})^2 \rangle = -\frac{4}{3} \epsilon^w r, \quad (2)$$

$$S_{3L}^z(r) \equiv \langle \delta w_L (\delta \mathbf{z})^2 \rangle = -\frac{4}{3} \epsilon^z r, \quad (3)$$

where  $\delta z_L$  and  $\delta w_L$  are longitudinal components of  $\delta \mathbf{z}$  and  $\delta \mathbf{w}$ ,  $\epsilon^w$  is the transfer rate of the  $\mathbf{w}$  field and  $\epsilon^z$  is the transfer rate of the  $\mathbf{z}$  field (see also [4]). If one now follows the analogy with the non-magnetized case

and assumes that all typical fluctuations are of the same size ( $\delta z_L \sim \delta w_L \sim \delta z \sim \delta w \sim \delta v \sim \delta b$ ) one derives  $\delta v_r \sim \delta b_r \propto r^{1/3}$ , which leads to the Kolmogorov scaling of the MHD turbulence spectrum.

The above results (2,3) are derived for the case of homogeneous and isotropic turbulence. However, they may be extended to the case of turbulence with a strong guiding field by the following argument. According to [2, 3], the requirement of homogeneity allows one to derive the following expressions in the inertial range of turbulence

$$\frac{\partial}{\partial r^i} \langle \delta z^i (\delta \mathbf{w})^2 \rangle = -4 \epsilon^w, \quad (4)$$

$$\frac{\partial}{\partial r^i} \langle \delta w^i (\delta \mathbf{z})^2 \rangle = -4 \epsilon^z. \quad (5)$$

The additional assumption of isotropy then yields relations (2,3). In the case of a strong guiding field, the variations of the fluctuations in the field perpendicular direction are much stronger than their field parallel variations so that the latter can be neglected in the inertial interval. The spatial derivatives in expressions (4, 5) can therefore be replaced by their field perpendicular parts, which leads to expressions of the form (2,3) in which the point separation vector  $\mathbf{r}$  lies in the field perpendicular direction.

The understanding of MHD turbulence with a strong guiding field is of importance since such a setting is believed to mimic the inertial range of turbulence where a guiding field is always present whether due to external sources or large-scale eddies (see, e.g., [5, 6, 7]). Recent high resolution numerical simulations of strongly magnetized turbulence reveal the field-perpendicular energy spectrum  $E(k_\perp) \propto k_\perp^{-3/2}$  (see [4, 7, 8, 9]). The numerical observations therefore seem to contradict the exact Politano-Pouquet relations (2, 3). This apparent contradiction motivated our interest in the problem.

In the present paper, we propose that the numerical results are reconciled with the Politano-Pouquet relations if one invokes the phenomenon of scale-dependent dynamic alignment. The essence of the phenomenon is that at each field-perpendicular scale  $r$  ( $\sim 1/k_\perp$ ) in the inertial range, typical shear-Alfvén velocity fluctuations ( $\delta \mathbf{v}_r$ ) and magnetic fluctuations ( $\pm \delta \mathbf{b}_r$ ) tend to align the directions of their polarizations in the field-perpendicular plane, and turbulent eddies become anisotropic in that plane. The alignment and anisotropy are stronger for smaller scales, with the alignment angle decreasing with the scale as  $\theta_r \propto r^{1/4}$ . This leads to the scaling of the velocity and magnetic fluctuations,  $\delta v_r \sim \delta b_r \propto r^{1/4}$ , and explains the observed energy spectrum,  $E(k_\perp) \propto k_\perp^{-3/2}$ . This effect was predicted analytically in [10, 11] and verified numerically in [12].

### DYNAMIC ALIGNMENT AND POLITANO-POUQUET RELATIONS

There are two possibilities for the dynamic alignment: the velocity fluctuation  $\delta \mathbf{v}_r$  can be aligned either with  $\delta \mathbf{b}_r$  or with  $-\delta \mathbf{b}_r$ . These two cases are presented in Fig. 1 and Fig. 2, respectively. By definition, the amplitudes of  $\delta \mathbf{v}_r$  and  $\delta \mathbf{b}_r$  are of the order of their typical, rms values. Let us determine which configuration provides the dominant contribution to the structure functions (2) and (3). It is easy to see from Fig. 1 and Fig. 2 that when  $\delta z_r \sim \delta w_r$ , both alignment configurations contribute to both structure functions (2) and (3). However, when the magnitudes  $\delta v_r$  and  $\delta b_r$  are very close to each other, i.e. when the corresponding magnitudes  $\delta z_r$  and  $\delta w_r$  are significantly different, the configuration in Fig. 1 provides the dominant contribution to the structure function (2), while that in Fig. 2 dominates the structure function (3).

Without loss of generality, we therefore consider in detail only the structure function  $S_{3L}^w(r)$ , defined in (2), and concentrate on the contribution provided by the configuration presented in Fig. 1. The directions of the vectors  $\delta \mathbf{v}_r$  and  $\delta \mathbf{b}_r$  are aligned within a small angle  $\theta_r$  in the field-perpendicular plane, in the y-direction, say, and their wave vectors are aligned in the field-perpendicular plane in the x-direction. The dominant contribution to the structure function (2) then comes from the situation in which the point-separation vector  $\mathbf{r}$  lies in the x-direction, since the variation of the fields is strongest in this direction. In this case, the longitudinal projection (i.e., x-component) of  $\delta \mathbf{z}$ ,  $\delta z_L$ , is smaller by a factor of order  $\theta_r$  than the typical value of  $\delta w_r$ . This introduces an extra factor  $\theta_r$  in the Politano-Pouquet correlation function (2), and one obtains

$$\langle \delta z_L (\delta \mathbf{w})^2 \rangle \sim \theta_r \delta v_r^3. \quad (6)$$

As we demonstrated in [10, 11, 12], the scale-dependent dynamic alignment  $\theta_r \propto r^{1/4}$  leads to the scaling of fluc-

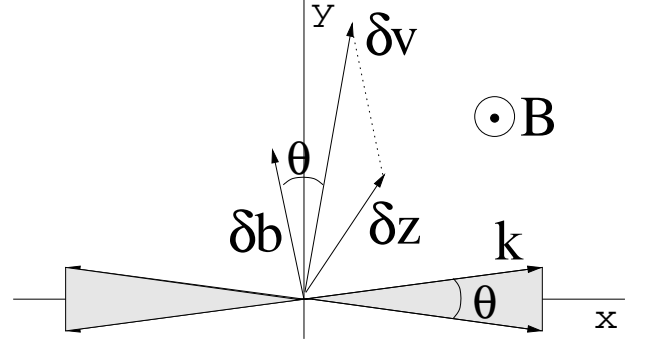


FIG. 1: Sketch of typical velocity and magnetic field fluctuations  $\delta \mathbf{v}_r$  and  $\delta \mathbf{b}_r$  aligned in the field-perpendicular plane within small angle  $\theta_r$ .

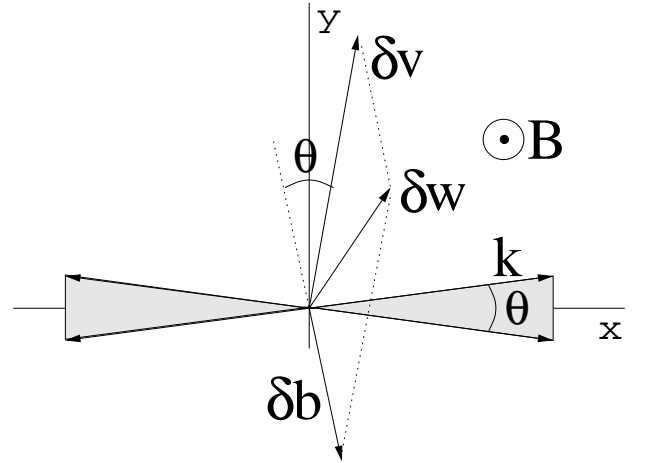


FIG. 2: Sketch of typical velocity and magnetic field fluctuations,  $\delta \mathbf{v}_r$  and  $\delta \mathbf{b}_r$ , aligned in the field-perpendicular plane such that the alignment angle  $\theta_r$  between  $\delta \mathbf{v}_r$  and  $-\delta \mathbf{b}_r$  is small.

tuating fields  $\delta v_r \sim \delta b_r \propto r^{1/4}$ , which explains the numerically observed field-perpendicular energy spectrum,  $E(k_\perp) \propto k_\perp^{-3/2}$ . Quite remarkably, by substituting these scalings into expression (6) we satisfy the scaling relation (2). Thus the earlier mentioned numerical findings are reconciled with the Politano-Pouquet relations if one invokes the phenomenon of scale-dependent dynamic alignment.

In the next section we verify relation (6) numerically. In particular, we measure the following structure functions

$$\tilde{S}_{3L}^w(r) = \langle |\delta z_L| (\delta \mathbf{w})^2 \rangle, \quad (7)$$

$$S_3^w(r) = \langle |\delta \mathbf{w}|^3 \rangle. \quad (8)$$

We use the absolute value of  $\delta z_L$  in calculating (7) to avoid cancellations and slow convergence caused by different signs of  $\delta z_L$ . If our idea expressed by (6) is correct, then  $\tilde{S}_{3L}(r) \sim \theta_r \delta v_r^3$  while  $S_3(r) \sim \delta v_r^3$  and therefore the ratio of these two functions should give us the alignment

angle  $\theta_r$ :

$$\theta_r = \tilde{S}_{3L}^w(r)/S_3^w(r). \quad (9)$$

This angle should scale with the point separation approximately as  $\theta_r \propto r^{1/4}$ .

## NUMERICAL RESULTS

We solve the incompressible MHD equations

$$\begin{aligned} \partial_t \mathbf{v} + (\mathbf{v} \cdot \nabla) \mathbf{v} &= -\nabla p + (\nabla \times \mathbf{B}) \times \mathbf{B} + \nu \Delta \mathbf{v} + \mathbf{f}, \\ \partial_t \mathbf{B} &= \nabla \times (\mathbf{v} \times \mathbf{B}) + \eta \Delta \mathbf{B}, \end{aligned} \quad (10)$$

where  $\mathbf{v}(\mathbf{x}, t)$  is the velocity field,  $\mathbf{B}(\mathbf{x}, t)$  the magnetic field,  $p$  the pressure,  $\mathbf{f}(\mathbf{x}, t)$  the external force, and  $\nu$  and  $\eta$  are the fluid viscosity and resistivity, respectively, using standard pseudospectral methods. An external magnetic field is applied in  $z$  direction with strength  $B_0 \approx 10$  measured in units of velocity. The periodic domain has a resolution of  $256^3$  mesh points and is elongated in the  $z$  direction, with aspect ratio  $1:1:B_0$ . The external force,  $\mathbf{f}(\mathbf{x}, t)$ , is chosen so as to drive the turbulence at large scales and it satisfies the following requirements: it has no component along  $z$ , it is solenoidal in the  $x-y$  plane, all the Fourier coefficients outside the range  $1 \leq k \leq 2$  are zero, the Fourier coefficients inside that range are Gaussian random numbers with unit variance and amplitude chosen so that the resulting *rms* velocity fluctuations are of order unity, and the individual random values are refreshed independently *on average* every turnover time of the large scale eddies. The Reynolds number is defined as  $Re = U_{rms}L/\nu$ , where  $L$  ( $\sim 1$ ) is the field-perpendicular box size,  $\nu$  is fluid viscosity, and  $U_{rms}$  ( $\sim 1$ ) is the rms value of velocity fluctuations. We restrict ourselves to the case in which magnetic resistivity and fluid viscosity are the same,  $\nu = \eta$ , with  $Re \approx 800$ . The system is evolved until a stationary state is reached (confirmed by observing the time evolution of the total energy of fluctuations). The data set consists of 40 samples that cover approximately 20 eddy turnover times.

To calculate the structure functions (7) and (8), we construct  $\delta \mathbf{z}(r) = \mathbf{z}(\mathbf{x} + \mathbf{r}) - \mathbf{z}(\mathbf{x})$  and  $\delta \mathbf{w}(r) = \mathbf{w}(\mathbf{x} + \mathbf{r}) - \mathbf{w}(\mathbf{x})$ , with  $\mathbf{r}$  in a plane perpendicular to  $\mathbf{B}_0$ . By definition,  $\delta z_L = \delta \mathbf{z}(r) \cdot \mathbf{r}/r$  and  $\delta w_L = \delta \mathbf{w}(r) \cdot \mathbf{r}/r$ . The average is then taken over different positions of the point  $\mathbf{x}$  in that plane, over all such planes in the data cube, and then over all data cubes.

The numerical calculation of expression (9) is shown in Fig. 3. We find  $\theta_r \propto r^{0.22 \pm 0.01}$ . We determined the accuracy of the scaling exponent by performing the same procedure with  $\mathbf{z}$  and  $\mathbf{w}$  interchanged, as is shown in Fig. 3. Ideally, i.e. for infinite averaging time, the two results should be the same. The slight difference in the two curves is a result of the finite size of the sample set. The agreement with the analytic prediction  $\theta_r \propto r^{0.25}$  is

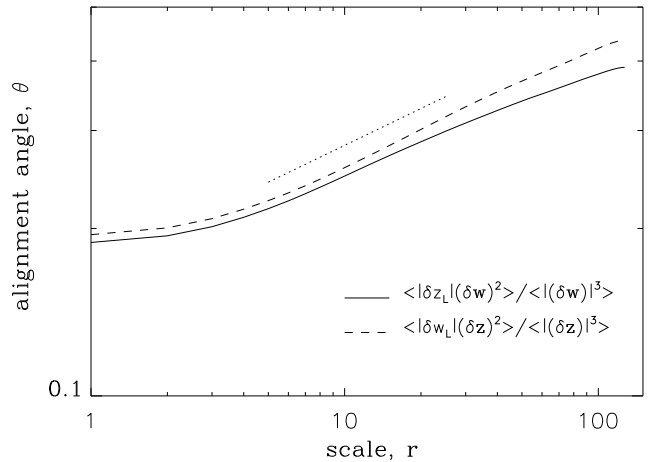


FIG. 3: The relative scaling of the structure functions  $\tilde{S}_{3L}^w(r)$  and  $S_3^w(r)$  expressed through the scaling of the alignment angle (9). The angle  $\theta_r$  is plotted vs scale  $r$ . The equivalent procedure with  $\mathbf{w}$  and  $\mathbf{z}$  interchanged yields a slightly different slope, which is a result of limited averaging time. This allows us to estimate the error of the measurements. The straight line has the slope 0.22, which is the mean slope of the two curves. The uncertainty in the slope value is about  $\pm 0.01$ .

good, given that the resolution of our simulations is not large enough to observe a well defined inertial interval, and that possible small intermittency corrections are not captured by our model. The result presented in (6) and numerically verified in Fig. 3 is the main result of our work.

## DISCUSSION AND CONCLUSION

Dynamic alignment is a known phenomenon of MHD turbulence [13, 14, 15, 16, 17]. However, in previous works it essentially meant that decaying MHD turbulence asymptotically reaches the so-called Alfvénic state where either  $\mathbf{v}(\mathbf{x}) \equiv \mathbf{b}(\mathbf{x})$  or  $\mathbf{v}(\mathbf{x}) \equiv -\mathbf{b}(\mathbf{x})$ , depending on initial conditions. It has been realized only recently [10, 11] that the effect is preserved in driven, stationary MHD turbulence, although in quite an interesting fashion. Fluctuations of  $\delta \mathbf{v}_r$  and  $\pm \delta \mathbf{b}_r$  tend to align their directions (although their magnitudes are not necessarily equal) and the alignment angle becomes *scale-dependent*, i.e., it decreases with scale as  $\theta_r \propto r^{1/4}$  [10, 11]. The first numerical observations of this phenomenon appeared in [12]. In the present paper we have demonstrated that this phenomenon is consistent with the exact relations known in MHD turbulence due to work by Politano and Pouquet [2, 3]. Our work thus serves as an additional argument in favor of the new model of MHD turbulence developed in [10, 11, 12].

Remarkably, both the ideas of the Alfvénic increase of

the interaction time, proposed by Iroshnikov and Kraichnan [18, 19], and of critically balanced field-parallel and field-perpendicular cascades, put forward by Goldreich and Sridhar [20], turn out to be consistent with the presented model. It is interesting, however, that the underlying physics of the model is qualitatively different from the physics originally envisaged in either [18, 19] or [20]. In contrast with [18, 19], in our model the turbulence is essentially anisotropic and strong at all scales. In contrast with [20], in our model the turbulent fluctuations are dynamically aligned, their nonlinear interaction is depleted, and the resulting spectrum is different from the prediction of [20].

MHD turbulence plays an essential role in astrophysical phenomena such as the solar wind (e.g. [21]), interstellar scintillation (e.g. [22]), cosmic ray acceleration, propagation, and scattering in the interstellar medium (e.g., [23, 24]), and thermal conduction in galaxy clusters (e.g. [25, 26, 27]). One of the most important consequences of the scale-dependent dynamic alignment is the energy spectrum of MHD turbulence, which becomes strongly anisotropic with respect to the local magnetic field. The field-perpendicular spectrum takes the form  $E(k_{\perp}) \propto k_{\perp}^{-3/2}$ . If one neglects many uncertainties, the spectrum of turbulence inferred from astrophysical observations is usually consistent with the Kolmogorov spectrum  $k^{-5/3}$ . However, there exist indications in favor of the spectrum  $-3/2$  in scintillation observations [28, 29]. Our theory may provide a natural explanation for such observations.

This work was supported by the NSF Center for Magnetic Self-Organization in Laboratory and Astrophysical Plasmas at the University of Wisconsin at Madison and the University of Chicago.

---

[1] Frisch, U., 1995, *Turbulence*. (Cambridge University Press, Cambridge).  
 [2] Politano, H. & Pouquet, A., Geophys. Res. Lett. 25 (1998) 273.

[3] Politano, H. & Pouquet, A., Phys. Rev. E **57** (1998) R21.  
 [4] Biskamp, D., 2003, *Magnetohydrodynamic Turbulence*. (Cambridge University Press, Cambridge).  
 [5] Milano, L. J., Matthaeus, W. H., Dmitruk, P., & Montgomery, D. C., Phys. Plasmas **8** (2001) 2673.  
 [6] Matthaeus, W. H., Ghosh, S., Oughton, S., & Roberts, D. A., J. Geophys. Res. **101** (1996) 7619.  
 [7] Maron, J., & Goldreich, P., ApJ **554** (2001) 1175.  
 [8] Müller, W.-C., Biskamp, D., & Grappin, R., Phys. Rev. E **67** (2003) 066302.  
 [9] Müller, W.-C. & Grappin, R., Phys. Rev. Lett., **95** (2005) 114502.  
 [10] Boldyrev, S., ApJ **626** (2005) L37.  
 [11] Boldyrev, S., Phys. Rev. Lett. **96** (2006) 115002.  
 [12] Mason, J., Cattaneo, F., & Boldyrev, S., Phys. Rev. Lett, submitted; astro-ph/0602382.  
 [13] Dobrowolny, M., Mangeney, A., & Veltri, P., Phys. Rev. Lett. **45** (1980) 144.  
 [14] Grappin, R., Frisch, U., Léorat, J., & Pouquet, A., Astron. Astrophys. **105** (1982) 6.  
 [15] Pouquet, A., Meneguzzi, M., & Frisch, U., Phys. Rev. A **33** (1986) 4266.  
 [16] Pouquet, A., Sulem, P. L., Meneguzzi, M., Phys. Fluids **31** (1988) 2635.  
 [17] Politano, H., Pouquet, A., Sulem, P. L., Phys. Fluids B **1** (1989) 2330.  
 [18] Iroshnikov, P. S., AZh, **40** (1963) 742; Sov. Astron, **7** (1964) 566.  
 [19] Kraichnan, R. H., Phys. Fluids, **8** (1965) 1385.  
 [20] Goldreich, P. & Sridhar, S., ApJ **438** (1995) 763.  
 [21] Goldstein, D. A. Roberts, D. A., & Matthaeus, W. H., Annu. Rev. Astron. Astrophys. **33** (1995) 283.  
 [22] Lithwick, Y. & Goldreich, P., ApJ **562** (2001) 279.  
 [23] Kulsrud, R. M., & Pearce, W. P., ApJ **156** (1969) 445.  
 [24] Wentzel, D. G., ARA&A **12** (1974) 71.  
 [25] Rechester, A. B. & Rosenbluth, M. N., Phys. Rev. Lett. **40** (1978) 38.  
 [26] Chandran, B.D.G. & Cowley, S.C., Phys. Rev. Lett. **80** (1998) 3077.  
 [27] Narayan, R. & Medvedev, M., ApJ **562** (2001) L129.  
 [28] Shishov, V. I., Smirnova, T. V., Sieber, W., Malofeev, V. M., Potapov, V. A., Stinebring, D., Kramer, M., Jessner, A., and Wielebinski, R., Astron. Astrophys. **404** (2003) 557.  
 [29] Smirnova, T. V., Gwinn, C. R., & Shishov, V. I., astro-ph/0603490.